Research Article

Investigation of Operating Conditions Effect on Dimethyl ether Production by Methanol

Amir Heidari[*], Mehdi Navaei Larimi , Zahra Mehdiabadi

Process Simulation and Modeling Laboratory (PSMlab), Faculty of Chemical, Petroleum and Gas Engineering, Semnan University, Semnan,

3513119111, Iran

A R T I C L E I N F O

A B S T R A C T

In this study, the process of dimethyl ether (DME) production from methanol (MeOH) was simulated. The UNIQUAC and Peng-Robinson equations were applied as the activity model and the equation of state in the simulation model, respectively. To evaluate the effect of operational parameters on DME production, the impact of reactor temperature and dimensions, distillate rate, and reflux ratio from two distillation columns was investigated. The results indicated that with an increase in the reactor residence time, a maximum conversion of 85% is achieved for all studied temperature ranges. Results showed that by increasing the first distillation column (T-10 column) feed flow rate from 130 kmol/h to 170 kmol/h, the purity of DME decreases by about 40%, but the recovery rate of DME increases by about 30%. Furthermore, changes in the reflux ratio of the T-10 column in the range of 0.35 to 0.8 showed a low effect on the DME purity and recovery. Also, it was observed that with an increase in the T-10 column distillate rate from 110 kmol/h to 130 kmol/h, the reactor conversion increased by about 7%. Upon raising the flow rate of the recycle stream from 50 kmol/h to 250 kmol/h, the reactor conversion and DME purity in the product stream decrease by about 45% and 20%, respectively. Finally, using the genetic algorithm (GA) method, the operational conditions were optimized to reach the maximum purity of DME in the final product. Results showed the reflux ratio of the second distillation column has the main effect on the enhancement of product DME purity.

* Corresponding author.
  E-mail address: amirheidari@semnan.ac.ir

1. Introduction

Dimethyl ether, also known as methoxymethane, is a colorless gas at standard temperature and pressure. At 25°C, it exhibits a vapor pressure of around 0.6 MPa and readily liquefies under low pressure [1]. DME is an eco-friendly fuel option due to its cleaner combustion compared to traditional fuels, resulting in lower emissions of NO_x, CO, and hydrocarbons. Additionally, DME has a low global warming potential compared to chlorofluorocarbons, which were traditionally used as coolants but are now banned. DME is also known for its stability, relatively non-toxic nature, and ease of storage [2, 3]. DME has several applications, including aerosol, fuel cell fuel, solvent, propellant, chemical feedstock, transportation fuel, or refrigerant. In recent years, there has been a shift in primary usage toward blending with liquefied petroleum gas (LPG). In addition, DME serves as a crucial feedstock for synthesizing a range of other products, such as dimethyl sulfate, methyl acetate, and light olefins [2]. Moreover, by using the Monsanto process, DME can be converted to acetic acid via carbonylation [4].

During the last few years, two methods have been employed for producing DME: direct [5-7] and indirect [8-14]. On the other hand, numerous studies have been conducted on the simulation and modeling of DME production. Bercic and Levec [8] conducted a simulation of an adiabatic fixed-bed reactor for the catalytic dehydration of methanol to DME. Their findings suggest that a model neglecting interfacial gradients could accurately predict DME production. The researchers also discovered intraparticle mass transfer controlled the rate-limiting step when using 3 mm γ-alumina pellets as the catalyst. Fazlollahnejad et al. [15] created a model for a bench-scale adiabatic reactor that was one-dimensional and steady-state, as well as pseudo-homogeneous. They compared the longitudinal temperature and conversion profiles predicted by this model with those measured experimentally in a bench-scale reactor. The maximum conversion rate reported was approximately 95.8% at 603.15 K with a weight hourly space velocity (WHSV) of 72.87 h^{-1}. The reactor was filled with 1.5 mm γ-Al_2O_3 pellets as a dehydration catalyst. Nasehi et al. [16] conducted a simulation of an industrial adiabatic fixed-bed reactor for DME production via MeOH dehydration under steady-state conditions. Their findings suggest that the distinction between one-dimensional and two-dimensional modeling in adiabatic fixed-bed reactors is insignificant. Farsi et al. [17] simulated an industrial reactor for DME synthesis that was equipped with a feed pre-heater. They developed a model based on a system of algebraic and partial differential equations utilizing the Bercic & Levec equation. The researchers investigated process controllability using dynamic simulations with a conventional feedback PID controller. The simulation results indicated that the model is reasonable, as it closely matched the available data from an industrial reactor. Yoon and Song

[18] conducted simulations of the reactor under steady-state conditions, employing a one-dimensional steady-state model of a heterogeneous catalyst bed. They compared the simulation findings with data acquired from a pilot-scale reactor. Additionally, the researchers evaluated the effectiveness factor for the catalyst pellets and derived concentration and temperature profiles along the height of the reactor catalyst bed. Farsi et al. [19] modeled a shell-and-tube fixed-bed reactor for the synthesis of DME and enhanced its output by fine-tuning the temperature profile along the reactor using a genetic algorithm. Yaseri and Shahrokhi [20] developed a model for an isothermal reactor designed to synthesize DME directly from syngas. The model was one-dimensional, steady-state, and pseudo-homogeneous. The effects of shell temperature, flow rate, and feed pressure on CO conversion were studied by them. Kumar and Srivastava [21] modified the model propounded by Mahecha-Botero et al. and used the modified model to simulate DME production in a fluidized-bed reactor. A simulation performed on an industrial adiabatic fixed-bed reactor for DME production revealed that the discrepancy between one-dimensional and two-dimensional models is minimal [22]. Khademi et al. [23] conducted steady-state heterogeneous modeling to assess the optimal operating conditions and improve the production of dimethyl ether and benzene in a thermally coupled reactor. Bai et al. [24] simulated the dimethyl ether synthesis process, utilizing the integrated parameters from the reaction kinetics model for methanol dehydration, the enhanced NRTL model for the liquid phase, and the PR model for the vapor phase. The simulation results were compared with the available data from a set of industrial production equipment, and the calculated and measured results were found to be satisfactory. Bakhtyari et al. [25] used a steady-state one-dimensional plug flow model to study the behavior of a catalytic heat-exchanger reactor assisted with two different membranes for methanol conversion to DME, methyl formate, and hydrogen. Babiker et al. [26] simulated the production of dimethyl ether from methanol to predict the compositions, the final production rate, and the distribution of the main components in the final product. Alshbuki et al. [27] conducted a simulation study for the production of DME from methanol. This simulation was based on the combined parameters of the reaction kinetics model for methanol dehydration reaction, the improved NRTL model of the liquid phase, and the PR model of the vapor phase. Despite the abundance of research studies on reactor simulation and distillation process modeling for DME production, the process simulation of DME synthesis from methanol dehydration appears to be infrequent.

In the current study, the process of DME production by the indirect synthesis method was simulated. In the first step, the simulation of the process was carried out in the base state, and then in the next step, the effects of operational parameters were investigated on the quality of

DME production. Finally, the operational conditions were optimized by the genetic algorithm method to achieve the highest purity of DME.

2. Process flow diagram of DME production

Figure 1 shows the DME production process flow diagram (PFD) [28] used in this research. The feed stream (Stream 1) comprises methanol and a small amount of water as an impurity and is introduced into the reactor at ambient conditions. The feed stream is pressurized by a pump (P-10) and combined with the reflux stream (Distillate T-20) from the second distillation column (T-20) with a high percentage of methanol. This mixture (Stream 3) is preheated to 220-250°C before entering the reactor. Since the reaction is exothermic, the heat from Stream 6 (reactor outlet stream) is utilized to increase the temperature of the reactor inlet stream (Stream 5). The reactor comprises tubes filled with a catalyst in which methanol is decomposed and DME and water are produced based on the following equation:
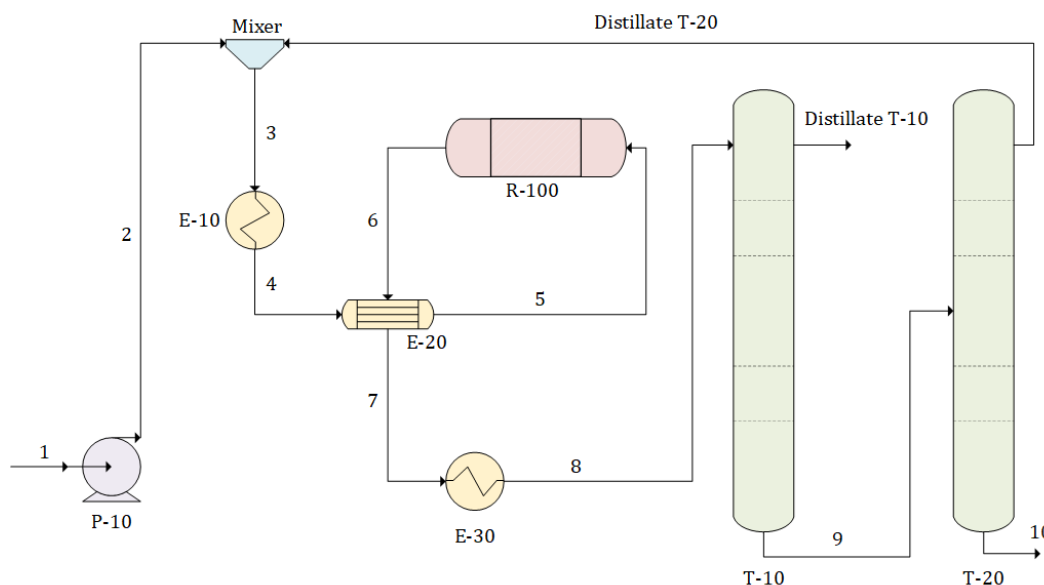
$$2\,CH_3OH \rightarrow CH_3OCH_3 + H_2O \tag{1}$$

Fig. 1. Dimethyl Ether production process diagram [28]

The reactor outlet stream (Stream 6) is initially cooled in the heat exchanger E-20 and then cooled again in the heat exchanger E-30 to reduce its temperature below 90°C, which is a suitable temperature for entering the first distillation column (T-10 column).

The distillate stream of the T-10 column comprises DME with high purity (Distillate T-10), and the T-10 bottom product (Stream 9) includes methanol with water.

Stream 9 enters the T-20 distillation column to separate methanol and water. High-purity water comes out of the system as the bottom product of the T-20 distillation column (Stream 10), and high-purity methanol is recycled from the top product of the distillation column (Distillate T-20) and mixed with the feed stream (Stream 1). In this paper, the DME process was simulated by the UNIQUAC and Peng-Robinson equations as the activity model and equation of state, respectively. Table 1 shows data on DME production streams at the base state [28]. During the simulation, the following assumptions were made: A) The efficiency of trays in the distillation column is 100%, B) Pressure drop in the streams was ignored, C) The flow regime in the reactor is plug flow.

Table 1. Flowsheet data for DME process at basic state [28]

Streams	1	2	3	4	5	6	8	Distillate -T10	9	10	Distillate -T20
Temperature (°C)	25	25	35.87	154	230	338	89	47	119.8	162.8	76.64
Pressure (bar)	1	15.5	15.5	15.1	14.7	13.9	10.45	10.4	7.52	7.6	7.4
Molar flow rate (kmol/h)	262.2	262.2	328.5	328.5	328.5	328.5	328.5	129.7	198.8	132.5	66.28
MeOH mole fraction	0.991	0.991	0.9394	0.939	0.939	0.174	0.174	0.0317	0.268	0.035	0.732
Water mole fraction	0.008	0.008	0.007	0.007	0.007	0.390	0.390	0	0.6449	0.964	0.006
DME mole fraction	0	0	0.052	0.052	0.052	0.435	0.435	0.9683	0.087	0	0.261

2.1. Reactor specifications and reactions rates

The dehydration reaction of methanol (Eq. (1)) is carried out using a catalytic tube reactor in the gas phase. The measured reactor is 4 meters long and includes 2000 tubes with an inner diameter of 9 cm that are filled with alumina (Al_2O_3) catalyst particles with a diameter of 5.4 mm. The reaction is carried out catalytically in terms of bed volume [29, 30]. The pressure drop across the length of the reactor is calculated using the Ergun equation:

$$\frac{\Delta P}{L} = \frac{150 \times \mu \times (1-\varepsilon)^2 \times U_0}{\varepsilon^3 \times d_p} + \frac{1.75 \times (1-\varepsilon) \times \rho \times U_0^2}{\varepsilon^3 \times d_p} \tag{2}$$

where ΔP represents the pressure drop across the reactor, μ stands for fluid viscosity, ε represents the void fraction, U_0 is the fluid velocity at the reactor entrance, ρ is the fluid density, and d_p is the diameter of catalyst particles. Alumina density is 1200 kg/m³, and the catalytic bed has a void fraction of $\varepsilon = 0.5$. The kinetic model of the reaction was given by Bercic and Levec [8], which can be seen in Eqs. (3)-(7).

$$R_{DME} = \frac{KK_m \left(C_{MeOH}^2 - \frac{C_W C_{DME}}{K_{fDME}}\right)}{(1 + 2 \times (K_{MeOH}C_{MeOH})^{0.5} + K_{Water}C_{Water})^4} \quad kmol/(kgcat \times s) \tag{3}$$

$$K = 874575 \times \exp\left(-71375.5/R_gT\right) \tag{4}$$

$$K_{MeOH} = 3 \times 10^{-4} \times \exp\left(16495.81/R_gT\right) \tag{5}$$

$$K_{Water} = 6 \times 10^{-7} \times \exp\left(31796.89/R_gT\right) \tag{6}$$

$$K_{fDME} = \exp\left(\frac{4019}{T} + 3.707 \times Ln(T) - 2.783 \times 10^{-3} \times T + 3.8 \times 10^{-7} \times T^2 \right. $$
$$\left. - 6.561 \times 10^4 \times 1/T^3 - 26.64\right) \tag{7}$$

where C_{MeOH}, C_W and C_{DME} represent the methanol, water and DME concentration respectively, R_g is the gas constant and T is temperature.

2.2. T-10 distillation column

The outlet stream from the reactor (Stream 6) enters the T-10 distillation column after being cooled to 85°C. This column has two outlet streams: the Distillate T-10 stream, which is the desired product and contains DME with small amounts of water and methanol as impurities; and Stream 9, which contains a high percentage of H_2O and MeOH with a low percentage of DME. Stream 9 is sent to the T-20 distillation column to separate the methanol and then mixed with the feed stream (Stream 2) for reuse through a reflux stream. The T-10 column has 22 trays (from top to bottom), and the feed enters the distillation column at tray 12. A total condenser is located at the top of the distillation column with a reflux ratio of 0.35.

2.3. T-20 Distillation column

Stream 9 from the bottom of the T-10 distillation column is sent to the T-20 distillation column. The T-20 column comprises 26 trays, and the feed stream enters at tray 14 with a reflux ratio of 1.7. This column has two outlet streams: the Distillate T-20 stream, which consists mostly of MeOH and DME with water as an impurity, and the bottom product of the T-20 distillation column (Stream 10), which contains a small amount of MeOH as an impurity and a high percentage of water, which exits the process.

3. Result and discussion

3.1. Validation

The simulation results of the current work were compared with reported data by Turton et al. [28]. The DME mole fraction, DME molar flow rate in the final product, and reactor performance were the studied parameters for validation. The results of this work showed less than a 2% error with Turton et al. [28] simulation data.

3.2. Effect of operational conditions on DME production efficiency

The main aim of the current study is to identify the factors that affect the DME process, including reactor conversion, DME purity, and recovery. Therefore, the following parameters were investigated to study their impact on the process performance:

1) Reactor residence time (reactor length) and reactor inlet temperature (Stream 5)
2) The flow rate of the Distillate T-10 stream and reflux ratio of the T-10 distillation column
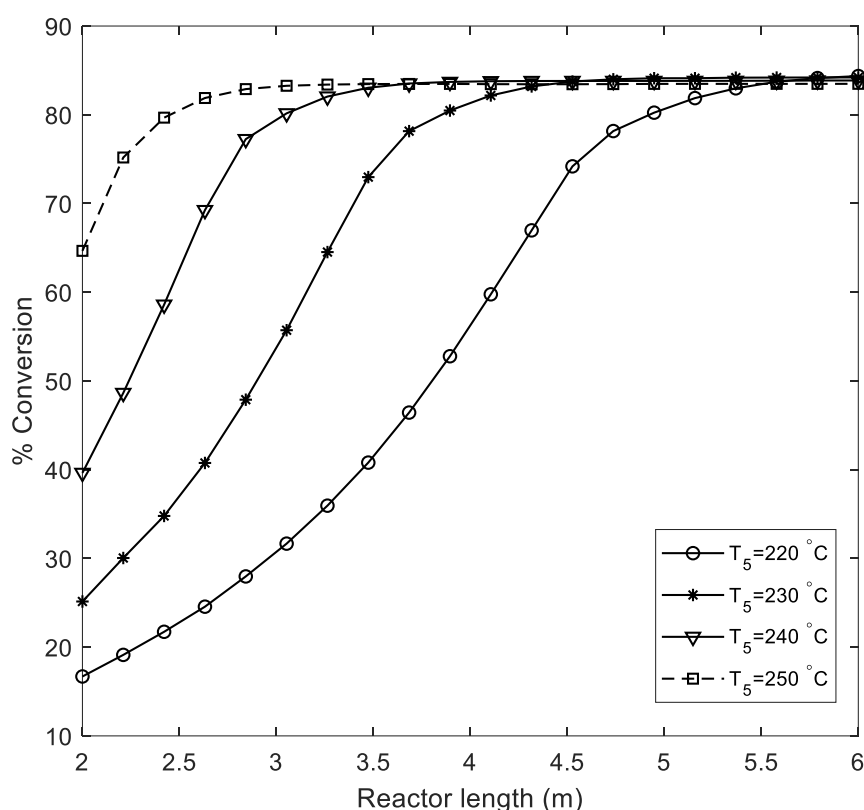3) The flow rate of the Distillate T-20 stream and reflux ratio of the T-20 distillation column

Fig. 2. Reactor conversion in terms of reactor length at different reactor inlet temperatures (Stream 5)

3.3. Effects of reactor residence time and reactor feed temperature (Stream 5)

3.3.1. Reactor conversion

To investigate the effect of reactor residence time in terms of reactor length on the reaction conversion, reactor length variations between 2 m and 6 m were chosen. With an increase in the reactor length, the residence time of methanol increases, and as a result, the methanol conversion increases in the reactor. Figure 2 illustrates methanol conversion in terms of reactor length at different reactor inlet temperatures. As shown in Fig. 2, at the lowest temperatures, a maximum reactor length of 6 m is required to reach the highest reaction conversion (about 85%). Additionally, with an increase in the temperature of the reactor feed (Stream 5), the maximum conversion of 85% occurs at a shorter reactor length. This can be attributed to the increase in the reaction rate that occurs with rising temperature, which allows for the maximum conversion percentage of DME production to be achieved in a short residence time (shorter reactor length).

3.3.2. Purity and recovery of DME in the Distillate T-10 stream

Figure 3 depicts the impact of reactor length and reactor feed stream (Stream 5) temperature on the DME mole fraction or DME purity in the Distillate T-10 (product) stream. As Fig. 2 shows, with an increase in the reactor length, reactor conversion increases owing to an increase in the residence time of the components in the reactor, and then reactor conversion becomes steady. As Fig. 3 shows, the maximum mole fraction of DME at different reactor lengths and temperatures is about $Y_{DME} = 0.98$. Also, an increase in the Stream 5 temperature (reactor inlet stream) provides the final conversion at a shorter length of the reactor. So, the high purity of DME in the Distillate T-10 can be achieved by an increase in the reactor length or reactor inlet temperature.
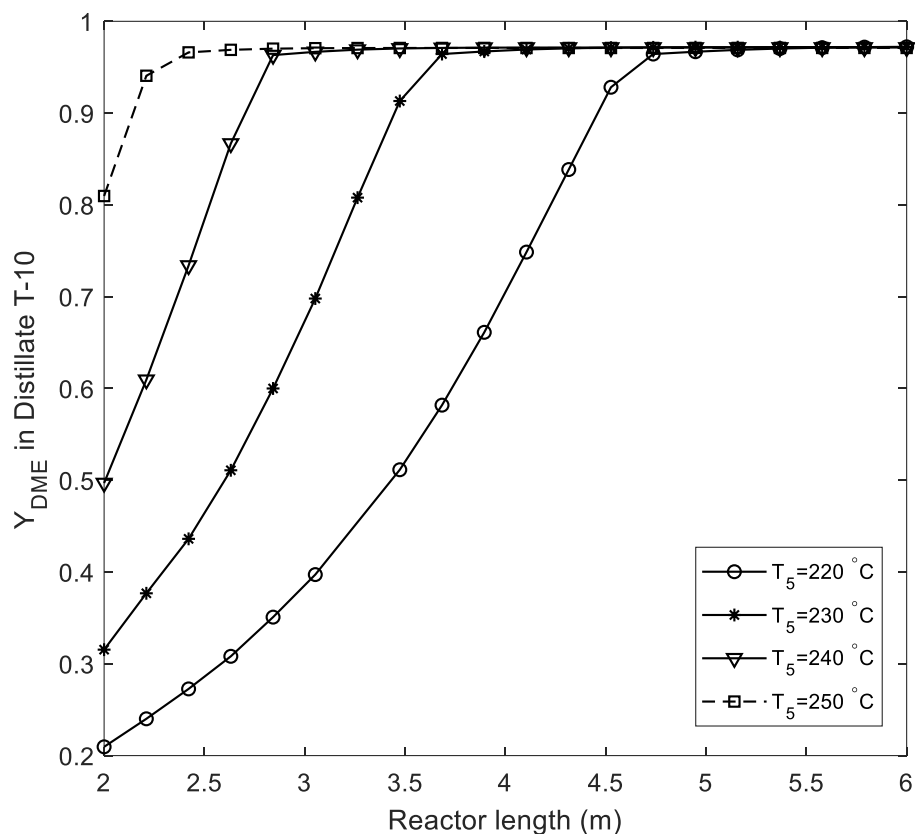
Fig. 3. DME molar fraction (DME purity) in Distillate T-10 stream in terms of reactor length at different temperatures of reactor inlet stream (Stream 5)

Figure 4 shows the effect of reactor length at different reactor inlet temperatures (Stream 5) on the DME recovery in the T-10 distillation column. As Fig. 4 depicts, DME recovery starts at its maximum level (100%) before decreasing and finally reaches a minimum value at different inlet stream (Stream 5) temperatures. At low residence times (small reactor length, Fig. 3), the purity of DME decreases in the reactor product. In this condition, the maximum DME recovery occurs in the T-10 column, Fig. 4. Also, it should be noted that maximum recovery of DME causes a reduction in DME purity in the Distillate T-10 stream (product stream, Fig. 3). On the other hand, as the reactor conversion increases with an increase in the reactor length, DME purity increases at the T-10 column inlet stream and Distillate T-10, but DME recovery decreases.
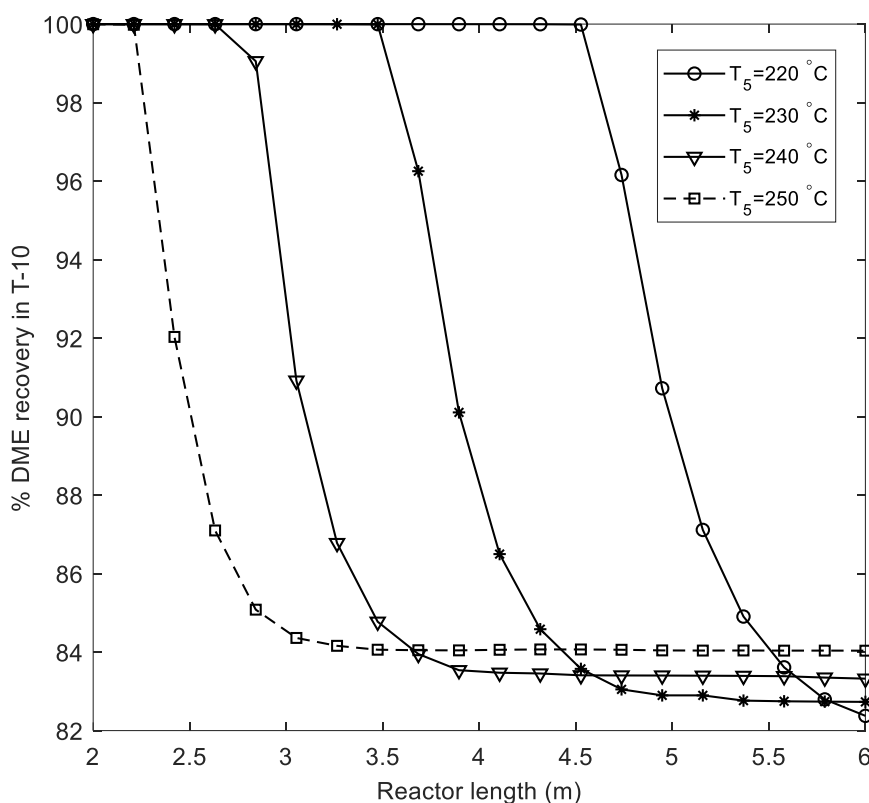
Fig. 4. DME recovery in the T-10 column in terms of reactor length at different temperatures of reactor inlet stream (Stream 5)

3.4. Effect of Distillate T-10 flow rate and reflux ratio of T-10 distillation column

3.4.1. Recovery and purity of DME in the Distillate T-10 stream

Figure 5 illustrates the purity of DME in the T-10 distillation column based on the molar flow rate of the Distillate T-10 stream at various reflux ratios of the T-10 column. The DME purity in the T-10 column is directly and indirectly influenced by the flow rate of the Distillate T-10 stream and the reflux ratio of the T-10 column. By altering the flow rate of the Distillate T-10 stream (direct effect), the purity of the DME in the Distillate T-10 stream changes.

The changes in the purity of DME and flow rate of the Distillate T-10 stream affect the performance of the T-20 distillation column. Subsequently, MeOH purity and liquid flow rate change in the Distillate T-20 stream. The Distillate T-20 stream is recycled to the process as reactor feed. Accordingly, reactor conversion is affected by the conditions of the Distillate T-20 stream, which leads to changes in the performance of the T-10 column, and the Distillate T-10 properties (indirect effect). With regard to Fig. 5, the mole fraction of DME has a constant value in the Distillate T-10 stream at low molar flows and then reduces for molar flows of more than 130 kmol/h.

In order to study the effect of the Distillate T-20 stream molar flow rate on the purity of DME in the Distillate T-10 stream, the MeOH purity should be studied in the Distillate T-20 stream (Fig. 6). As MeOH purity decreases in the recycled stream (Distillate T-20 stream), the DME production decreases in the reactor. So, the purity (mole fraction) of DME decreases in the reactor product and consequently in the Distillate T-10 stream (more details about the effect of Distillate T-10 flow rate on the MeOH purity in Distillate T-20 stream (recycled stream) are presented in section 3.3.2). According to Fig. 5, for reflux ratios greater than 0.65, the graphs almost coincide, and it can be said that the mole fraction of DME in the Distillate T-10 stream at a constant flow rate and a reflux ratio greater than 0.65 is not strongly dependent on the reflux ratio.
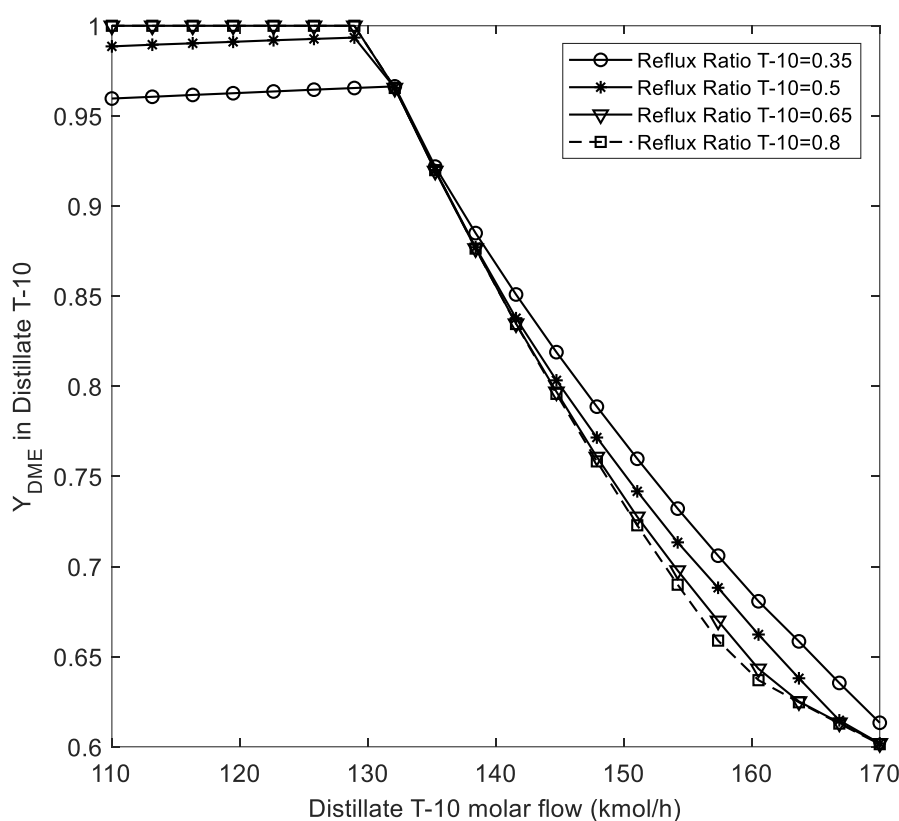

Fig. 5. DME molar fraction in Distillate T-10 stream in terms of the molar flow rate of Distillate T-10 stream at different reflux ratios of the T-10 column

3.4.2. MeOH purity in the Distillate T-20 stream and reactor conversion

Figure 6 shows the variation of MeOH purity (mole fraction) in the Distillate T-20 stream with respect to the molar flow rate of the Distillate T-10 stream at different reflux ratios of the T-10 column. To fully understand the behavior in Fig. 6, the presented results in Figs. 5 and 7 should be discussed.

As the flow rate of the Distillate T-10 increases, the mole fraction of DME in Distillate T-10 remains constant at first (Fig. 5), while DME recovery increases in the T-10 distillation column (Fig. 7).

This leads to an increase in methanol purity in the bottom product of the T-10 distillation column (Stream 9) and subsequently an increase in the methanol purity in Distillate T-20 (Fig. 6). However, when the Distillate T-10 molar flow rate passes 130 kmol/h, DME purity in Distillate T-10 decreases (Fig. 5), while DME recovery is at its maximum value (Fig. 7). This means that more methanol exits from the Distillate T-10 stream and, consequently, the bottom product of the T-10 column (Stream 9) has a lower concentration of methanol. Consequently, methanol purification declines in the Distillate T-20 stream (Fig. 7).
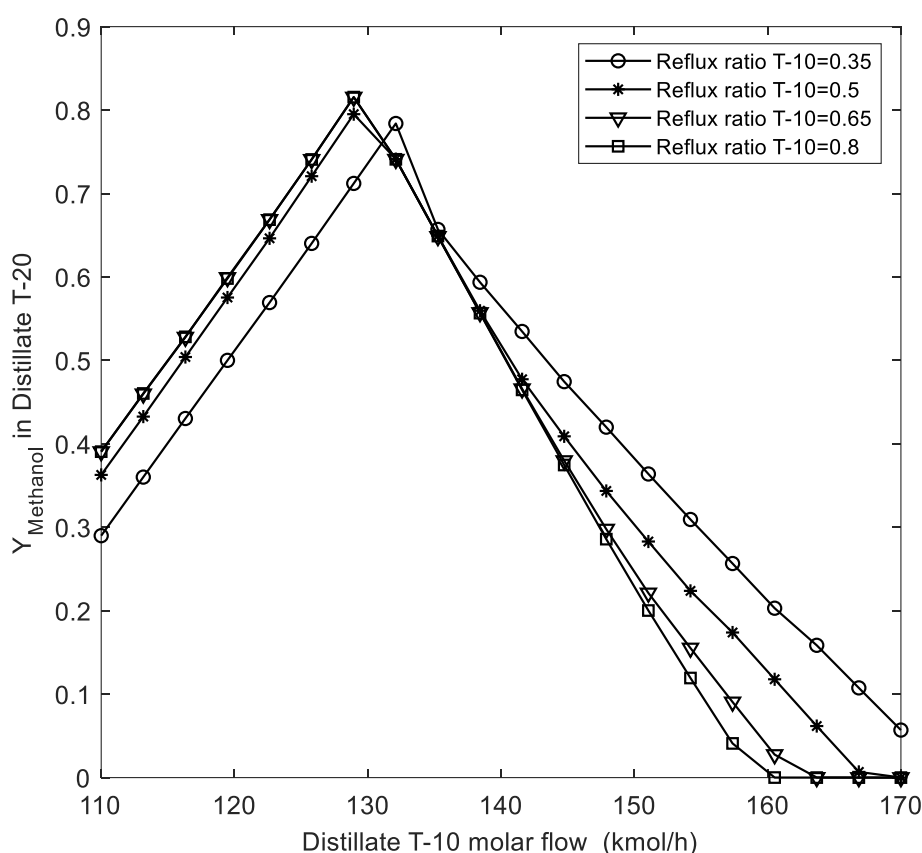

Fig. 6. Methanol mole fraction in Distillate T-20 stream in terms of the molar flow rate of Distillate T-10 stream at different Reflux ratios of the T-10 column
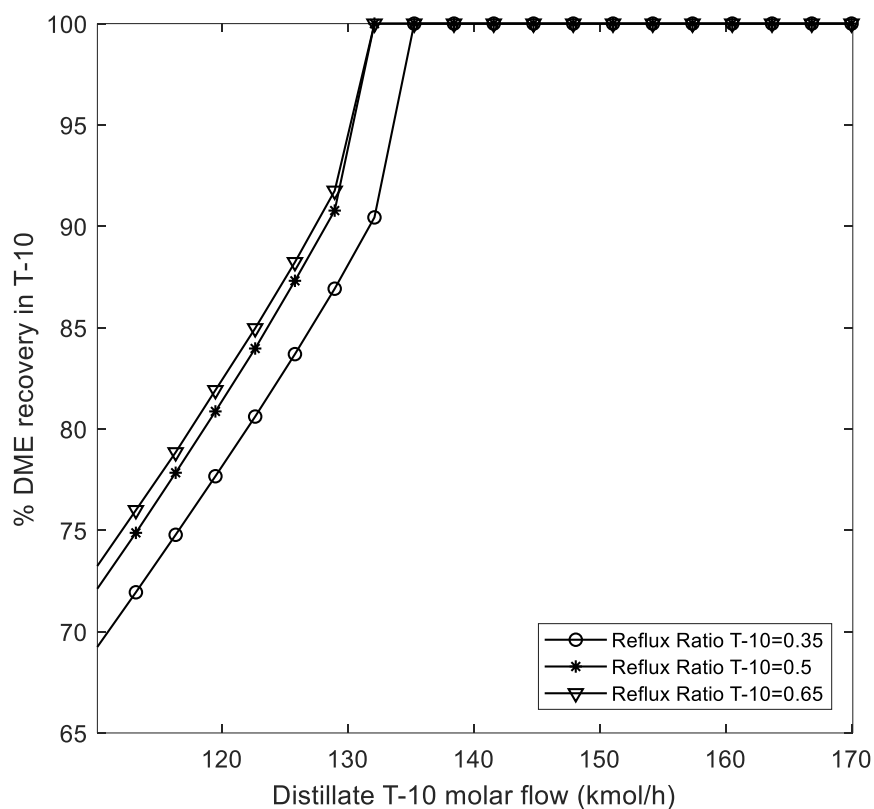
Fig. 7. DME recovery in the T-10 distillation column in terms of the molar flow rate of Distillate T-10 stream at different Reflux ratios of the T-10 column
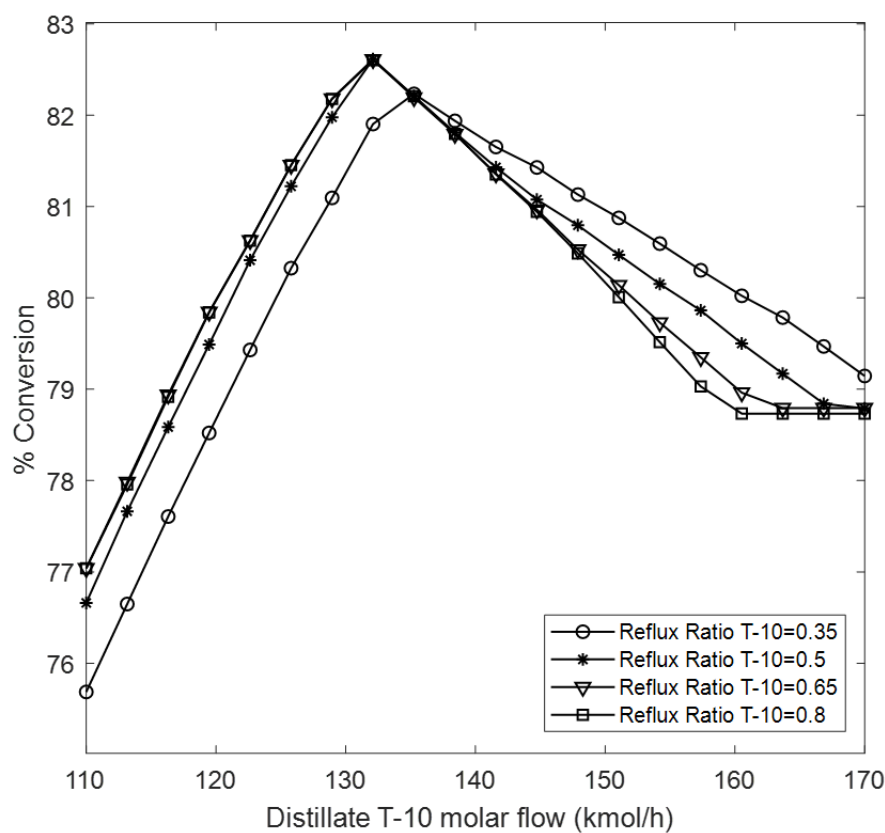

Fig. 8. Reactor conversion in terms of the molar flow rate of Distillate T-10 stream at different Reflux ratios of T-10 distillation column

Figure 8 shows the effect of the Distillate T-10 molar flow on the MeOH conversion in the R-100 reactor at different reflux ratios of the T-10 distillation column. According to the reaction kinetics of Eq. (3), the MeOH concentration plays the main role in the reactor conversion. So, by comparing the trend of MeOH purity in Distillate T-20 in Fig. 6 with MeOH conversion in Fig. 8, it is observed that the trend of reactor conversion follows methanol purity in the Distillate T-20 stream at different reflux ratios of the T-10 distillation column.

3.5. Effect of Distillate T-20 stream flow rate and reflux ratio of T-20 column

3.5.1. Reactor conversion

Figure 9 illustrates the conversion of the reactor for the molar flow rate of the Distillate T-20 stream at various reflux ratios of the T-20 distillation column. As Fig. 1 shows, the Distillate T-20 stream is recycled and combined with the feed stream (Stream 1 (or 2)) before entering the reactor. As depicted in Fig. 9, for all reflux ratios of the T-20 column, there is a decrease in reactor conversion as the molar flow rate of Distillate T-20 increases. This reduction in conversion is attributed to an increase in the reactor feed flow rate, which results in a decrease in the residence time and a reduction in the reactor conversion.
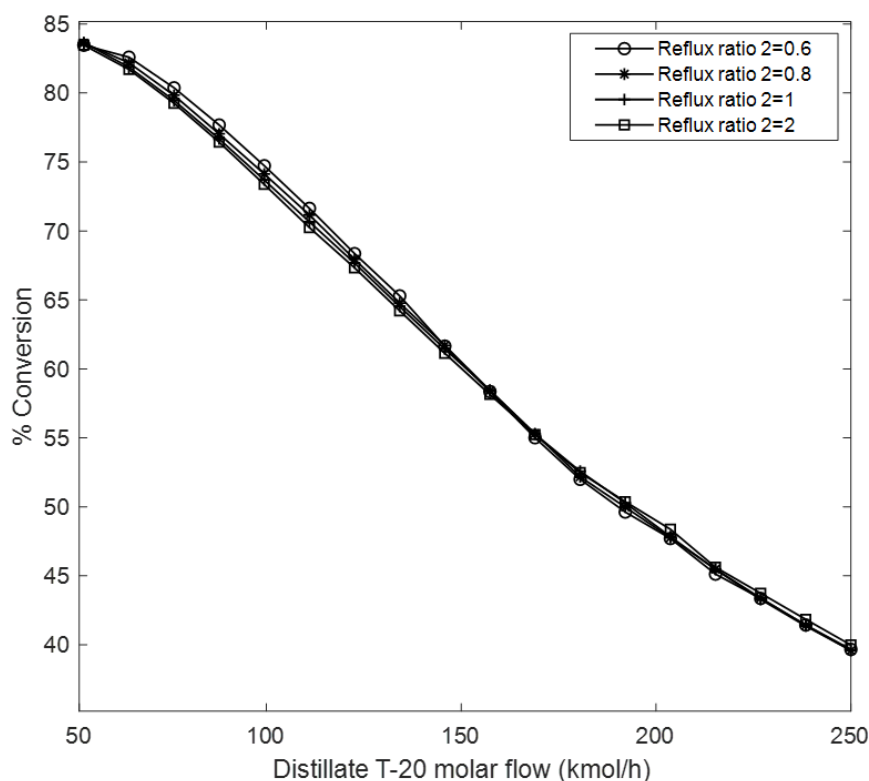

Fig. 9. Reactor conversion in terms of Distillate T-20 stream molar flow rate in different reflux ratios of T-20 distillation column

3.5.2. DME purity in the Distillate T-10 stream

Figure 10 shows the effect of the Distillate T-20 stream flow rate on the DME mole fraction in the Distillate T-10 stream at different reflux ratios of the T-20 distillation column. To study the effect of the Distillate T-20 molar flow on the purity of DME in the Distillate T-10 stream, the reactor conversion should be studied. According to Fig. 9, as the Distillate T-20 flow rate increases, reactor conversion reduces, which leads to a decrease in the purity of DME in the reactor output stream (or T-10 distillation column feed). So, as Fig. 10 shows, the DME mole fraction reduces with an increase in the Distillate T-20 molar flow due to a reduction in the DME purity at the T-10 distillation column feed.
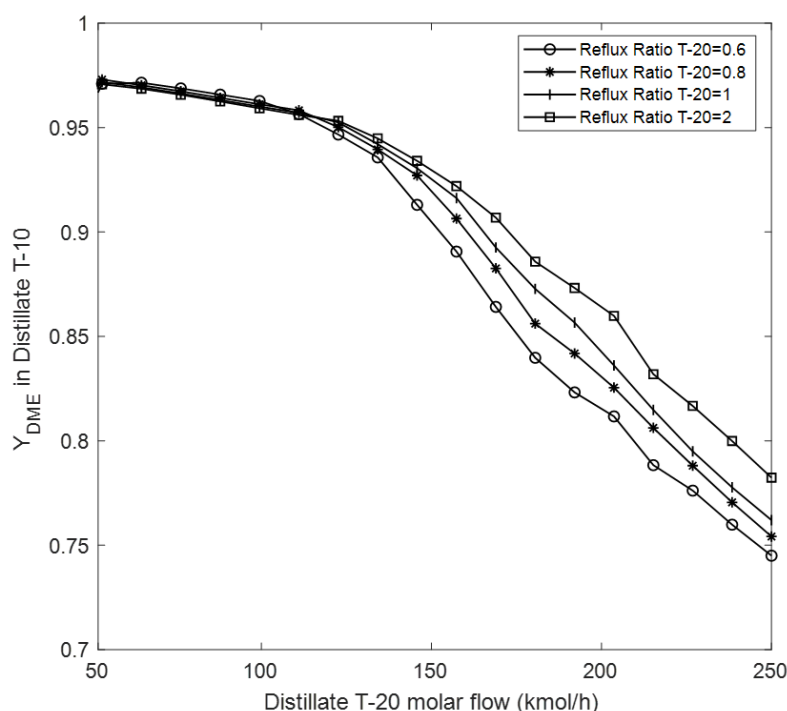

Fig. 10: DME molar fraction in Distillate T-10 stream in terms of the molar flow rate of Distillate T-20 at different reflux ratios of T-20 column

4. Optimization of DME purity at product stream (Distillate T-10 stream)

To increase the purity of DME in the Distillate T-10 stream (product stream), the GA method was used to enhance DME purity in the product. The GA objective function was defined as the maximization of the DME mole fraction in the Distillate T-10 stream. The adjusted parameters and constraints to enhance DME purity in the product stream are defined in Table 2. The Gaussian function and scattered crossover method were used to produce mutation children and to combine two individuals, or parents, to form a crossover child for the next generation, respectively. Also, the GA calculation stops if the average relative change in the best fitness function is less than 10^{-6}.

Table 2. GA adjusted parameters with constrains

Parameter	Low bound	High bound
Stream 5 temperature (℃)	220	250
Stream 8 temperature (℃)	60	90
Distillate T-10 molar flow ($kmol/h$)	110	170
Distillate T-20 molar flow ($kmol/h$)	40	240
Reflux ratio of T-10 column	0.2	3
Reflux ratio of T-20 column	0.2	3

Table 3 shows the values of parameters before and after optimization. According to Table 3, the mole fraction of DME at the optimized product stream (Distillate T-10) increased from 0.968 to 0.999. According to the results, the reflux ratio of the T-10 column has the main effect on the maximization of DME purity. The optimized value of the T-10 column reflux ratio increased by about 59% compared to the initial value. Also, it should be noted that although the purity of DME increases in the Distillate T-10 stream, the flow rate of the Distillate T-10 decreases from 129.7 kmol/h to 121.6 kmol/h.

Table 3. GA optimized value for enhancement of DME purity in Distillate T-10 stream

Parameter	Basic value	Optimized value
Stream 5 temperature (℃)	230	232.40
Stream 8 temperature (℃)	89	89.04
Distillate T-10 molar flow ($kmol/h$)	129.7	121.61
Distillate T-20 molar flow ($kmol/h$)	66.26	40.01
Reflux ratio of T-10 column	0.36	0.55
Reflux ratio of T-20 column	1.70	1.46
DME mole fraction (purity)	0.968	0.999

5. Conclusion

This research involved the simulation and optimization of the DME production process from methanol. The studies revealed that increasing the reactor residence time as a function of reactor length from 2 to 6 meters at varying operating temperatures (220, 230, 240, and 250°C) shows a maximum efficiency of 85% with a maximum purity of 98% for DME. Also, results showed that at a temperature of 220°C, the minimum required reactor length was 6 meters, and at a temperature of 250°C, the minimum reactor length to achieve the highest efficiency was about 3 meters.

An analysis of increasing the Distillate T-10 flow rate on DME purity in the Distillate T-10 stream from 110 kmol/h up to 130 kmol/h showed there are no significant changes in DME purity. However, with the increasing Distillate T-10 flow rate up to 170 kmol/h, DME purity decreased by up to 60%. Also, the results indicated that increasing the reflux ratio of the T-10 distillation column from 0.35 to 0.8 at a Distillate T-10 flow rate of less than 130 kmol/h increases DME purity in the process. But, with the increasing Distillate T-10 flow rate up to 170 kmol/h, the DME purity decreased. The effect of the Distillate T-10 stream's molar flow on DME recovery showed that complete recovery occurs at flow rates of more than 135 kmol/h at different reflux ratios of the T-10 distillation column. An analysis of the T-20 distillation column performance revealed that an increase in the Distillate T-20 stream (recycle stream) flow rate from 50 to 250 kmol/h reduces reactor conversion by about 45%. Also, due to the reduction in reactor conversion, the purity of DME decreased by about 20% in the final product (Distillate T-10 stream). According to the studied parameters in this work, the GA method was implemented in the model to maximize DME purity in the final product (Distillate T-10 stream). Results showed that the reflux ratio of the second distillation column (T-10 column) has the main effect on the maximization of DME purity in the final product. Future work on this subject can be conducted to simulate new direct and indirect DME production and process optimization.

Nomenclature

C	Concentration (m^3/s)
d_p	Particle diameter (m)
P	Pressure (Pa)
R	Reaction rate $(kmol/(kg_{cat}.s))$
R_g	Gas constant $(J/mol.K)$
T	Temperature (K)
U_0	Velocity at the reactor entrance (m/s)
ε	Void fraction
μ	Viscosity $(Pa.s)$
ρ	Density (kg/m^3)

Conflicts of Interest

The author declares that there is no conflict of interest regarding the publication of this article.

References

[1] T. Ogawa, N. Inoue, T. Shikada, Y. Ohno, Direct dimethyl ether synthesis, J. Nat. Gas Chem., 12 (2003) 219-227.

[2] Z. Azizi, M. Rezaeimanesh, T. Tohidian, M.R. Rahimpour, Dimethyl ether: A review of technologies and production challenges, Chem. Eng. Process.: Process Intensif., 82 (2014) 150-172.

[3] D. Good, J. Francisco, A. Jain, D.J. Wuebbles, Lifetimes and global warming potentials for dimethyl ether and for fluorinated ethers: CH3OCF3 (E143a), CHF2OCHF2 (E134), CHF2OCF3 (E125), Geophys. Res. Atmos., 103 (1998) 28181-28186.

[4] C. Fortin, N. Gianfolcaro, R. Gonzalez, J. Lohest, A. Lonneux, A. Kesnelle, N. Siliki, T. Peiffer, R. Renson, C. Schmitz, Dimethyl ether, A review of production processes and a modeling of the indirect route, Liege University, PROJ0012-1, (2020).

[5] T. Takeguchi, K.-i. Yanagisawa, T. Inui, M. Inoue, Effect of the property of solid acid upon syngas-to-dimethyl ether conversion on the hybrid catalysts composed of Cu–Zn–Ga and solid acids, Appl. Catal. A Gen., 192 (2000) 201-209.

[6] F. Ramos, A.D. De Farias, L.E.P. Borges, J. Monteiro, M.A. Fraga, E.F. Sousa-Aguiar, L.G. Appel, Role of dehydration catalyst acid properties on one-step DME synthesis over physical mixtures, Catal. Today, 101 (2005) 39-44.

[7] K.-W. Jun, H.-S. Lee, H.-S. Roh, S.-E. Park, Highly water-enhanced H-ZSM-5 catalysts for dehydration of methanol to dimethyl ether, B. Korean Chem. Soc., 24 (2003) 106-108.

[8] G. Bercic, J. Levec, Catalytic dehydration of methanol to dimethyl ether. Kinetic investigation and reactor simulation, Ind. Eng. Chem. Res., 32 (1993) 2478-2484.

[9] M. Xu, D.W. Goodman, A. Bhattacharyya, Catalytic dehydration of methanol to dimethyl ether (DME) over Pd/Cab-O-Sil catalysts, Appl. Catal. A Gen., 149 (1997) 303-309.

[10] F. Yaripour, F. Baghaei, I. Schmidt, J. Perregaard, Catalytic dehydration of methanol to dimethyl ether (DME) over solid-acid catalysts, Catal. Commun., 6 (2005) 147-152.

[11] M. Xu, J.H. Lunsford, D.W. Goodman, A. Bhattacharyya, Synthesis of dimethyl ether (DME) from methanol over solid-acid catalysts, Appl. Catal. A Gen.,149 (1997) 289-301.

[12] A. Eliassi, L. Savadkoohi, A. Kargari, Effects of various process parameters on temperature profile of adiabatic fixed bed reactor for production of dimethyl ether (DME) from methanol, Chem. Eng. Commun., 194 (2007) 1495-1502.

[13] B. Voss, F. Joensen, J.B. Hansen, Preparation of fuel grade dimethyl ether, Google Patents, 1999.

[14] E. Taranci, Dimethyl ether production from methanol over silica-alumina catalysts, Graduate School of Engineering and Sciences, Izmir Institute of Technology, Izmir, Turkey, 2021.

[15] M. Fazlollahnejad, M. Taghizadeh, A. Eliassi, G. Bakeri, Experimental study and modeling of an adiabatic fixed-bed reactor for methanol dehydration to dimethyl ether, Chin. J. Chem. Eng., 17 (2009) 630-634.

[16] S. Nasehi, R. Eslamlueyan, A. Jahanmiri, Simulation of DME reactor from methanol, Proceedings of the 11th chemical engineering conference, Iran, Kish Island, 2006.

[17] M. Farsi, R. Eslamloueyan, A. Jahanmiri, Modeling, simulation and control of dimethyl ether synthesis in an industrial fixed-bed reactor, Chem. Eng. Process.: Process Intensif., 50 (2011) 85-94.

[18] I.H. Kim, S. Kim, W. Cho, E.S. Yoon, Simulation of commercial dimethyl ether production plant, Comput. Aided Chem. Eng., 28 (2010) 799-804.

[19] M. Farsi, A. Jahanmiri, R. Eslamloueyan, Modeling and optimization of MeOH to DME in isothermal fixed-bed reactor, Int. J. Chem. React. Eng., 8 (2010).

[20] E. Yasari, M. Shahrokhi, H. Abedini, Modeling, simulation and control of a tubular fixed-bed dimethyl ether reactor, Chem. Biochem. Eng. Q., 24 (2010) 415-423.

[21] M. Kumar, V.C. Srivastava, Simulation of a fluidized-bed reactor for dimethyl ether synthesis, Chem. Eng. Technol., 33 (2010) 1967-1978.

[22] S.Y.g. Hosseini, M.R.K. Nikou, Modeling of industrial fixed bed reactor to produce dimethyl ether from methanol and determination of optimum operating conditions, Am. J. Sci., 8 (2012).

[23] M. Khademi, M. Farsi, M. Rahimpour, A. Jahanmiri, DME synthesis and cyclohexane dehydrogenation reaction in an optimized thermally coupled reactor, Chem. Eng. Process.: Process Intensif., 50 (2011) 113-123.

[24] Z. Bai, H. Ma, H. Zhang, W. Ying, D. Fang, Process simulation of dimethyl ether synthesis via methanol vapor phase dehydration, Pol. J. Chem. Technol., 15 (2013) 122–127.

[25] A. Bakhtyari, M. Parhoudeh, M.R. Rahimpour, Optimal conditions in converting methanol to dimethyl ether, methyl formate, and hydrogen utilizing a double membrane heat exchanger reactor, J. Nat. Gas Sci. Eng., 28 (2016) 31-45.

[26] H. Babiker, B. Karma, A.A. Mohammed, AspenHysys Simulation of Methanol to Dimethylether DME, Int. J. Eng. Trends Technol., 46 (2017) 214-220.

[27] E.H. Alshbuki, M.M. Bey, A.A. Mohamed, Simulation production of dimethylether (DME) from dehydration of methanol using aspen hysys, Envir., 2 (2020) 3.

[28] R. Turton, J.A. Shaeiwitz, D. Bhattacharyya, W.B. Whiting, Analysis, synthesis, and design of chemical processes, 5th edition, Prentice Hall, Boston, 2018.

[29] K. Dagde, U. Harry, Modeling of a Tubular Fixed-Bed Reactor for the Production of Dimethyl Ether Using Alumina Catalyst, Int. J. Chem. Eng., 3 (2016) 23-34.

[30] M. Farsi, Dynamic modeling and controllability analysis of DME production in an isothermal fixed bed reactor, Chem. Eng. Res. Bull., 17 (2015) 40-51.